Evidence of TeV halos around millisecond pulsars

Dan Hooper[1,2,*] and Tim Linden[3,†]

[1]*Theoretical Astrophysics Group, Fermi National Accelerator Laboratory, Batavia, Illinois 60510, USA*
[2]*Department of Astronomy & Astrophysics and the Kavli Institute for Cosmological Physics (KICP), University of Chicago, Chicago, Illinois 60637, USA*
[3]*Stockholm University and The Oskar Klein Centre for Cosmoparticle Physics, Alba Nova, 10691 Stockholm, Sweden*

(Received 6 April 2021; revised 27 February 2022; accepted 28 April 2022; published 16 May 2022)

Using data from the HAWC gamma-ray telescope, we have studied a sample of 37 millisecond pulsars (MSPs), selected for their spindown power and proximity. From among these MSP, we have identified four which favor the presence of very high-energy gamma-ray emission at a level of $(2\Delta \ln \mathcal{L})^{1/2} \geq 2.5$. Adopting a correlation between the spindown power and gamma-ray luminosity of each pulsar, we performed a stacked likelihood analysis of these 37 MSPs, finding that the data supports the conclusion that these sources emit very high-energy gamma-rays at a level of $(2\Delta \ln \mathcal{L})^{1/2} = 4.24$. Among sets of randomly selected sky locations within HAWC's field-of-view, less than 1% of such realizations yielded such high statistical significance. Our analysis suggests that MSPs produce very high-energy gamma-ray emission with a similar efficiency to that observed from the Geminga TeV-halo, $\eta_{\rm MSP} = (0.39 - 1.08) \times \eta_{\rm Geminga}$. This conclusion poses a significant challenge for pulsar interpretations of the Galactic Center gamma-ray excess, as it suggests that any population of MSPs potentially capable of producing the GeV excess would also produce TeV-scale emission in excess of that observed by HESS from this region. Future observations by CTA will be able to substantially clarify this situation.

DOI: 10.1103/PhysRevD.105.103013

I. INTRODUCTION

Observations by the High Altitude Water Cherenkov (HAWC) Observatory have identified bright, multi-TeV emission from the regions surrounding the nearby Geminga and Monogem pulsars [1–4]. The spectra and intensity of these "TeV halos" (also known as gamma-ray or ICS halos in the literature) indicate that roughly ∼10% of these pulsars' spindown power is converted into very high-energy electron-positron pairs. The angular extent of this emission (corresponding to roughly ∼25 pc in the range of energies measured by HAWC) indicates that cosmic-ray propagation is far less efficient in the vicinity of these pulsars than it is elsewhere in the interstellar medium [5–9] (for further discussion, see Refs. [10–16]).

In the time since HAWC's discovery of TeV halos around Geminga and Monogem, it has become increasingly clear that such emission is a nearly universal feature of middle-aged pulsars (i.e., those with ages on the order of $\sim 10^5$ yr). In particular, a large fraction of the sources detected by HAWC [1,2,17,18] (and many detected by HESS [19,20]) are spatially coincident with a pulsar. Moreover, there is a strong correlation between the spindown power of these pulsars and their observed gamma-ray luminosities. Recently, the HAWC Collaboration has produced a catalog of nine gamma-ray sources that have been detected at energies above 56 TeV [21], all of which are located within 0.5° of a known pulsar, most of which are very young ($\sim 10^4$ yrs) and exhibit exceptionally high spindown fluxes (defined as the spindown power divided by the distance square). At present, all indications are that young and middle-aged pulsars are generically surrounded by spatially extended TeV halos, powered by the rotational kinetic energy of these objects, and which produce their observed gamma-ray emission through the inverse Compton scattering of very high-energy electrons and positrons on the surrounding radiation field [10–12].

A more open question is whether recycled pulsars, with millisecond-scale periods, are also surrounded by TeV halos. Although no TeV sources are currently associated with a millisecond pulsar (MSP), this is not surprising given that MSPs are typically fainter multiwavelength sources with lower-spindown powers compared to the most energetic young pulsars which compose the majority of leptonic TeV sources. From a theoretical perspective, it is generally anticipated that MSPs (like young pulsars) should produce bright multi-TeV emission within their magnetospheres [22–24], as their light curves indicate that the production of very high-energy electron-positron pairs

*dhooper@fnal.gov
†linden@fysik.su.se

is efficient [22]. On the other hand, models of young and middle-aged pulsars generally include subsequent TeV-scale electron acceleration at the position of the pulsar wind nebula termination shock, a process which may only occur in the most powerful MSPs [25,26]. Additionally, it is unclear whether or not diffusion is inhibited in the regions surrounding MSPs, as it is observed to be around young and middle-aged pulsars [27,28].

The question of whether MSPs generate TeV halos is important not only in terms of our understanding of the particle acceleration associated with these objects, but also with respect to the excess of GeV-scale gamma-ray emission that has been observed from the region surrounding the Galactic Center. The spectrum, morphology, and intensity of this excess agrees well with the predictions for annihilating dark matter particles [29,30]. Alternatively, it has also been proposed that this excess emission could originate from a large population of unresolved MSPs, highly concentrated in the innermost volume of the Galaxy [31–33]. If it were confirmed that MSPs produce TeV halos (or other TeV-scale emission) at a level similar to young and middle-aged pulsars, measurements by HESS could be used to constrain the inner galaxy's MSP population to an abundance below that required to generate the GeV excess, potentially ruling out an MSP origin and providing significant support for the dark matter hypothesis.

In an earlier study [34], we used an online tool released for public use by the HAWC Collaboration, based on the HAWC observatory's first 507 days of data (corresponding to the data set used to construct the 2HWC catalog [2]), to search for evidence of very high-energy gamma-ray emission from MSPs. To this end, we performed an analysis of 24 MSPs within HAWC's field-of-view, identifying 2.6–3.2σ evidence that these objects produce diffuse very high-energy gamma-ray emission consistent with TeV halo models. We found that these systems exhibit a similar efficiency (defined as the ratio of very high-energy gamma-ray emission to spindown power) to that required to explain the multi-TeV emission observed from Geminga, Monogem, and other middle-aged and young pulsars.

In this paper, we revisit and expand upon this approach using an updated version of this online tool[1] to study the HAWC data taken over its first 1523 days of operation (corresponding to the dataset used to construct the 3HWC catalog [1]). Although the 3HWC catalog does not contain any sources that have been associated with an MSP [1], the approach pursued here allows us to look for TeV halos that do not necessarily meet the HAWC catalog's criteria of 5σ statistical significance. Using the 3HWC Survey Tool, we make use of a larger collection of high-spindown power MSPs, utilize updated distance measurements, and take advantage of the larger HAWC dataset. We find that this data supports the conclusion that MSPs emit very high-energy gamma-rays, and suggests that they produce this emission with a similar efficiency to that observed from the Geminga TeV-halo, $\eta_{\rm MSP} = (0.39 - 1.08) \times \eta_{\rm Geminga}$. This conclusion is difficult to reconcile with pulsar interpretations of the Galactic Center gamma-ray excess, as it indicates that any MSP population potentially responsible for the GeV excess would also produce TeV-scale emission at a level exceeding that observed from the region by HESS.

II. ANALYSIS METHOD

In our analysis, we have included all MSPs with periods below 50 ms found within the Australia Telescope National Facility (ATNF) pulsar catalog version 1.64[2] [35] that are located within HAWC's field-of-view ($-20° < \delta < 50°$), have a characteristic age greater than 1 Myr (defined as $t_c \equiv P/2\dot{P}$ where P is the observed period of the MSP and $\dot{P}$ is the derivative of this period, measured as a gradual slowing of the MSP spin as a function of time), and that exhibit a spindown flux greater than $\dot{E}/d^2 > 5 \times 10^{33}$ erg/kpc^2/s. The 37 MSPs that meet these requirements are shown in Table I, along with the values of their spindown power, distance, and spindown flux. We note that our spindown flux cutoff does not define any physical boundary, and it would be reasonable to include a sample with slightly more or fewer MSPs. However, we stress that the dimmer MSPs in our sample are not expected to produce observable emission if the efficiency is approximately uniform from pulsar-to-pulsar. Moreover, our joint-likelihood algorithm (which assumes a Geminga-like efficiency for each pulsar) would not be significantly affected if an MSP with a small spin-down flux unexpectedly had bright TeV emission (because our Geminga-like model could not fit an unexpectedly high TeV flux from such a source without overpredicting the TeV flux from MSPs with higher spindown powers). Thus, the lower cutoff of our MSP population has an extremely small effect on our results.

For each of these MSPs, we have used the 3HWC Survey Tool to determine the test statistic (TS) for the hypothesis that there is a source of very high-energy gamma rays with a spectral slope of -2.5 in a given direction of the sky. We note that this dataset, provided publicly by the HAWC collaboration, is the same reduced dataset used by the HAWC collaboration in the 3HWC catalog. The public release of this dataset it is crucial for our study, but it unfortunately restricts the user to an analysis at 7 TeV with a local spectrum of $E^{-2.5}$ as well as morphological choices

[1] https://data.hawc-observatory.org/datasets/3hwc-survey/coordinate.php

[2] https://www.atnf.csiro.au/research/pulsar/psrcat/index.html?version=1.64

TABLE I. The 37 known millisecond pulsars in HAWC's field-of-view with a spindown flux ($\dot{E}/d^2$) greater than 5×10^{33} erg/kpc^2/s [35]. In addition to the spindown power and distance to each pulsar, in the rightmost column we show the statistical significance (the square root of the test statistic) in favor of very high-energy gamma-ray emission as detected by HAWC using their online 3HWC Survey Tool. The four MSPs with $(\mathrm{TS})^{1/2} > 2.5$ are shown in blue.

Pulsar Name	$\dot{E}$ (erg/s)	Dist. (kpc)	$\dot{E}/d^2$ (erg/kpc^2/s)	$(\mathrm{TS})^{1/2}$
J0605 + 3757	9.3×10^{33}	0.215	2.01×10^{35}	−1.02
J1400 − 1431	9.7×10^{33}	0.278	1.26×10^{35}	−1.04
J1231 − 1411	1.8×10^{34}	0.420	1.02×10^{35}	−0.02
J1737 − 0811	4.3×10^{33}	0.206	1.01×10^{35}	−0.16
J1939 + 2134	1.1×10^{36}	3.500	8.98×10^{34}	3.34
J1710 + 4923	2.2×10^{34}	0.506	8.59×10^{34}	−0.62
J1959 + 2048	1.6×10^{35}	1.400	8.16×10^{34}	2.12
J2214 + 3000	1.9×10^{34}	0.600	5.28×10^{34}	0.33
J1843 − 1113	6.0×10^{34}	1.260	3.78×10^{34}	0.15
J1300 + 1240	1.9×10^{34}	0.709	3.78×10^{34}	−0.59
J1744 − 1134	5.2×10^{33}	0.395	3.33×10^{34}	−0.95
J0030 + 0451	3.5×10^{33}	0.325	3.31×10^{34}	2.55
J1023 + 0038	5.7×10^{34}	1.368	3.05×10^{34}	2.56
J2234 + 0944	1.7×10^{34}	0.769	2.87×10^{34}	0.80
J0218 + 4232	2.4×10^{35}	3.150	2.42×10^{34}	1.56
J0613 − 0200	1.3×10^{34}	0.78	2.14×10^{34}	0.06
J0337 + 1715	3.4×10^{34}	1.300	2.01×10^{34}	0.25
J1741 + 1351	2.3×10^{34}	1.075	1.99×10^{34}	2.64
J2339 − 0533	2.3×10^{34}	1.100	1.90×10^{34}	−0.35
J0621 + 2514	4.9×10^{34}	1.641	1.82×10^{34}	1.62
J0034 − 0534	3.0×10^{34}	1.348	1.65×10^{34}	0.10
J2042 + 0246	5.9×10^{34}	0.640	1.44×10^{34}	−0.67
J1719 − 1438	1.6×10^{33}	0.341	1.38×10^{34}	−0.56
J1921 + 1929	8.1×10^{34}	2.434	1.37×10^{34}	0.62
J1643 − 1224	7.4×10^{33}	0.740	1.35×10^{34}	0.66
J0023 + 0923	1.6×10^{34}	1.111	1.30×10^{34}	1.33
J2234 + 0611	1.0×10^{34}	0.971	1.06×10^{34}	−0.23
J1911 − 1114	1.2×10^{34}	1.070	1.05×10^{34}	−0.02
J1745 − 0952	5.0×10^{32}	0.226	9.79×10^{33}	−1.97
J2256 − 1024	3.7×10^{34}	2.083	8.53×10^{33}	0.45
J1630 + 3734	1.2×10^{34}	1.187	8.52×10^{33}	−0.59
J2017 + 0603	1.3×10^{34}	1.399	6.64×10^{33}	−0.37
J1622 − 0315	8.1×10^{33}	1.141	6.22×10^{33}	−0.51
J2043 + 1711	1.5×10^{34}	1.562	6.15×10^{33}	−0.72
J0751 + 1807	7.3×10^{33}	1.110	5.92×10^{33}	−2.09
J2302 + 4442	3.9×10^{33}	0.859	5.29×10^{33}	−0.01
J0557 + 1550	1.7×10^{34}	1.834	5.05×10^{33}	0.14

of a point source, or a Gaussian distribution with extensions of 0.5°, 1.0°, 2.0 °. By restricting the template in this way, the HAWC collaboration was able to perform systematic studies of cosmic-ray contamination and background uncertainties in order to verify source determination in this catalog, as discussed in detail in Ref. [1].[3] The test statistic is defined in terms of the likelihood as $\mathrm{TS} \equiv 2 \ln \Delta\mathcal{L}$ and, in the absence of any gamma-ray sources, the TS will be distributed according to a χ^2 distribution with one degree-of-freedom. The quantity $(\mathrm{TS})^{1/2}$ then corresponds to the pretrials significance in favor of a gamma-ray source being present in a given direction.

The online HAWC Survey tool can be used to determine the TS value for four different spatial templates, which we select for each pulsar based on its distance. This consists of picking an angular position in right ascension and declination for each pulsar, and selecting a spatial model to retrieve the $(\mathrm{TS})^{1/2}$ of each source. For our Monte Carlo simulations, we downloaded the underlying dataset available at the same website to automate the procedure of picking random source coordinates.

Operating under the assumption that typical TeV halos have a radius of ∼20–50 pc (in the range of energies measured by HAWC),[4] we adopt the pointlike template for pulsars with $d > 2$ kpc, the 0.5° extension template for 0.75 kpc $< d <$ 2 kpc, the 1° template for 0.375 kpc $< d <$ 0.75 kpc, and the 2° template for $d <$ 0.375 kpc. The square root of the test statistic for each of the 37 MSPs in our sample is reported in the rightmost column of Table I. Those entries which report a negative value for $(\mathrm{TS})^{1/2}$ represent directions of the sky which feature a statistical preference for a gamma-ray source with a negative normalization, likely resulting from an oversubtraction of the gamma-ray background.

In our previous study, in order to avoid regions of the sky that are contaminated by nearby gamma-ray sources, we considered only those MSPs that are more than 2° from any point-like source, and more than 2° from the edge of any extended source in the 2HWC catalog. Given the significantly larger number of sources in the 3HWC catalog (65, compared to 39 in the 2HWC catalog), such a cut would now remove several of the MSPs in our sample from consideration. With this in mind, we have adopted a cut designed to prevent any leakage greater than $\Delta\mathrm{TS} \gtrsim 1$ from any known source. Given that HAWC's point spread function is approximately ∼0.5° over the energy range

[3]While the spectral index measured for Geminga's TeV halo is consistent with the value of −2.5 adopted in the 3HWC Survey Tool, Monogem's spectral index is somewhat harder, ~ -2.0.

[4]Because cosmic-ray diffusion and leptonic energy losses (through synchrotron and inverse-Compton scattering) are highly energy-dependent processes, we expect the spatial extension of TeV halos to be highly energy dependent. For typical diffusion models (Kolmogorov/Kraichnan) we expect the faster leptonic cooling as at high energies to outpace the faster diffusion, leading to TeV halos which become smaller at high energies. This result is supported by potential observations of TeV halos at GeV-energies in Fermi-LAT data, with models indicating spatial extensions that may exceed HAWC measurements by more than an order of magnitude [15,36].

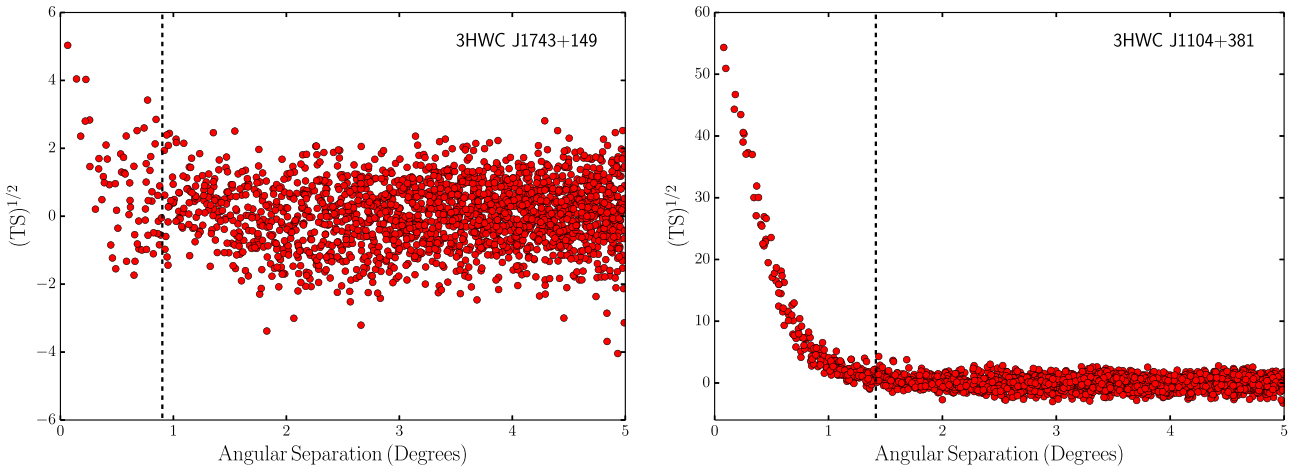

FIG. 1. The value of $(\mathrm{TS})^{1/2}$ found using the 3HWC Survey Tool in random sky locations near the faint HAWC source 3HWC J1743 + 149 (TS = 25.9), and the bright HAWC source 3HWC J1104 + 381 (TS = 3025.3). In removing any MSP from our analysis that is located within $0.5° \times [\ln(\mathrm{TS}_{\mathrm{3HWC}})]^{1/2}$ of any source in the 3HWC catalog (corresponding to the vertical dashed lines), we significantly limit the potential for contamination from this collection of sources.

of interest, this cut requires us to remove from our sample any MSPs that are located less than $0.5° \times [\ln(\mathrm{TS}_{\mathrm{3HWC}})]^{1/2}$ from any source in the 3HWC catalog, where $\mathrm{TS}_{\mathrm{3HWC}}$ is the test statistic of the source as reported by the HAWC collaboration. This cut removes from our analysis any MSP that is within 0.9° of the faintest 3HWC sources (*ie.* those with $\mathrm{TS} \simeq 25$), or within 1.6° of the brightest 3HWC source (the Crab Nebula). The impact of this cut is illustrated in Fig. 1, for the representative HAWC sources 3HWC J1743 + 149 and 3HWC J1104 + 381. Although this cut does not remove from our analysis any of the 37 MSPs listed in Table I, it will impact later stages of our analysis.

III. RESULTS

From among the 37 MSPs considered in our analysis, we have identified four with $(\mathrm{TS})^{1/2} \geq 2.55$. Under the assumption that the background is Gaussian, the chance probability of identifying four such sources is 0.16%, corresponding to a statistical significance 2.95σ. This is consistent with the results presented in our earlier analysis [34]. While this result is already interesting, it is potentially quite conservative, in that it weights all MSPs equally, regardless of their predicted gamma-ray flux (based on their spindown power and proximity).

In Table II, we show additional results for each of the 4 known millisecond pulsars in Table I with $(\mathrm{TS})^{1/2} > 2.5$, providing the value of $(\mathrm{TS})^{1/2}$ that is obtained when using each of the four spatial templates included in the online 3HWC Survey Tool. We note that for two of these sources, the best fit TS value is consistent with the prediction for the source extension given by our TeV halo model (based on the observed extent of Geminga, rescaled for distance). For J1023 + 0038, a point-source extension is favored to the 0.5° extension predicted by our models, though the significance of this difference is at $\mathrm{TS} < 1$. The fourth source, J1939 + 2134 shows significant evidence for extension despite having a distance of 3.5 kpc which would indicate that it is likely to be a point source in our model. We note that mismodeling may be a more significant issue for this source as it lies on the galactic plane and only ∼6° from a bright HAWC source 3HWC J1928 + 178. This is particularly true for extended spatial templates, which can include distant emission from nearby bright sources. However, an investigation of the 3HWC residuals (using the 3HWC interactive tool) near this source indicates that the PS model is unlikely to be affected by contamination from 3HWC J1928 + 178, as there are several "nodes" with TS = 0 that lie between the MSP and the nearby source, which indicates that there is not clear leakage from the 3HWC source into the PS determination of our MSP.

TABLE II. The 4 known millisecond pulsars in Table I with $(\mathrm{TS})^{1/2} > 2.5$, showing the results that are obtained when using each of the 4 spatial templates included in the online 3HWC Survey Tool. The numbers in bold represent the results that are obtained when using the template as selected based on the measured distance to the pulsar. We additionally show the characteristic age and binary status (Y/N) of each system, finding values that are typical for MSPs.

Pulsar	$(\mathrm{TS})^{1/2}_{\mathrm{PS}}$	$(\mathrm{TS})^{1/2}_{0.5°}$	$(\mathrm{TS})^{1/2}_{1°}$	$(\mathrm{TS})^{1/2}_{2°}$	Age (Myr)	Bin
J1939 + 2134	**3.34**	4.77	7.83	10.26	235	N
J0030 + 0451	0.068	1.08	2.21	**2.55**	7580	N
J1023 + 0038	3.12	**2.56**	0.19	−0.26	3860	Y
J1741 + 1351	1.09	**2.64**	2.16	1.58	1960	Y

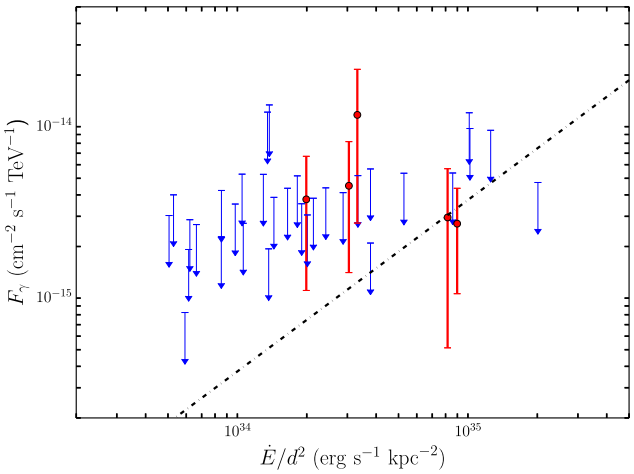

FIG. 2. The gamma-ray fluxes (evaluated at 7 TeV) of the 37 MSPs in our sample as determined using the 3HWC Survey Tool, and as a function of the spindown power, $\dot{E}/d^2$. For the 32 of these pulsars without any significant detection (those with $(\mathrm{TS})^{1/2}$ less than 2), we show the 2σ upper limit on the flux (blue). For each of the five sources with $(\mathrm{TS})^{1/2} > 2$, we plot the 1σ confidence interval on the gamma-ray flux (red). The black line represents the gamma-ray flux predicted under the assumption that each pulsar generates a TeV halo with the same efficiency as Geminga.

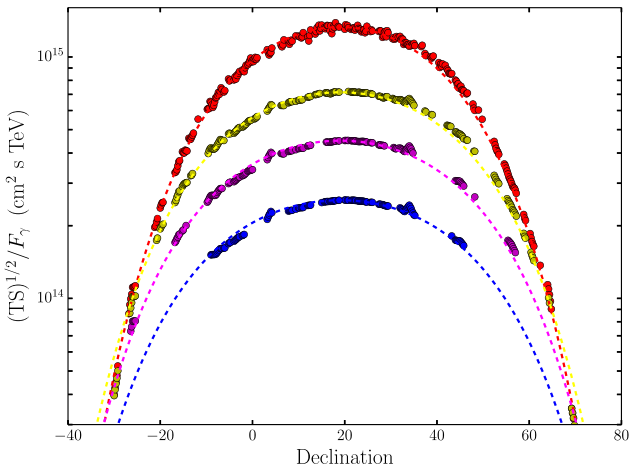

FIG. 3. The relationship between $(\mathrm{TS})^{1/2}/F_\gamma$ and declination as found using the 3HWC Survey Tool on random sky locations (points). From top-to-bottom, the different colors correspond to the results obtained using the point source template, the 0.5° extended template, the 1° extended template, and the 2° extended template. The dashed lines represent our polynomial fits to these results.

We note that the other three high-TS sources (with the exception of J1023 + 0038) do not lie in regions close to the galactic plane, with galactic latitudes of $b = -57.61$ (J0030 + 0451), $b = 45.78$ (J1023 + 0038) and $b = 21.64$ (J1741 + 1351), respectively. While it is difficult to build a latitude distribution out of only four sources, we note that this distribution is similar to what one might expect if galactic latitude did not play a significant role in determining MSP TS values. Finally, we note that two of the four bright MSPs are isolated systems, which is slightly unlikely (p-value 12.5%) given that only 6 of the 37 systems in our sample are isolated. The age distribution of our bright MSPs, on the other hand, is relatively consistent with the distribution of MSP ages in our sample, which typically have ages of several Gyr. We note that J1939 + 2134 is the youngest system in the sample, but there are also two other systems with ages below 1 Gyr.

In Fig. 2, we plot the gamma-ray fluxes (evaluated at 7 TeV) of the 37 MSPs in our sample as a function of $\dot{E}/d^2$, as determined using the 3HWC Survey Tool. For 32 of these pulsars (those with $(\mathrm{TS})^{1/2} < 2$), we show the 2σ upper limits on their flux. For each of the five sources with $(\mathrm{TS})^{1/2} > 2$, we plot the 1σ confidence interval. The black line in Fig. 2 represents the gamma-ray flux that is predicted under the assumption that each pulsar generates a TeV halo with the same efficiency as Geminga (i.e., that each pulsar has the same integrated gamma-ray flux above 0.1 TeV per unit spindown power as Geminga). In this regard, we have adopted here the following parameters for Geminga: $\dot{E} = 3.25 \times 10^{34}$ erg/s, $d = 0.19$ kpc [35], and $dN_\gamma/dE_\gamma = 4.87 \times 10^{-14}\,\mathrm{TeV}^{-1}\,\mathrm{cm}^{-2}\,\mathrm{s}^{-1} \times (E_\gamma/7\,\mathrm{TeV})^{-2.23}$ [2]. We note that, within the context of this Geminga-like model, individual MSPs may be detectably bright either due to the fact that they have an intrinsically high spin-down power, or due to the fact that they are particularly close to Earth. Additionally, we note that for our standard Geminga-like model, the vast majority of MSPs should not be individually detected, as the current 2σ flux upper limits typically exceed the expected luminosity for most of our systems by a factor of 5–10.

The fact that 5 of the 18 highest spindown power MSPs within HAWC's field-of-view have yielded 2σ or higher evidence of gamma-ray emission is suggestive, but by no means overwhelming. If this population of sources has an approximately universal Geminga-like efficiency for gamma-ray emission, however, we should expect a joint analysis of these sources to provide a much more powerful test of this hypothesis. With this in mind, we have used the 3HWC Survey tool to calculate the likelihood that each of the 37 MSPs in our sample produces a very high-energy gamma-ray flux that is proportional to their spindown power, allowing the overall normalization of this proportionality to float.

We note that the 3HWC Survey Tool does not report negative values for fluxes, even when preferred by the data. Fortunately, there is reliable relationship between the quantity $(\mathrm{TS})^{1/2}/F_\gamma$ and declination, which we use to determine the best-fit and limiting values of F_γ in these instances (see Fig. 3). For each spatial extension template, we model this relationship as $\log_{10}[(\mathrm{TS})^{1/2}/F_\gamma] = A + B\delta^2 + C\delta^4 + D\delta^6$, fitting each coefficient to the results of the 3HWC Survey Tool.

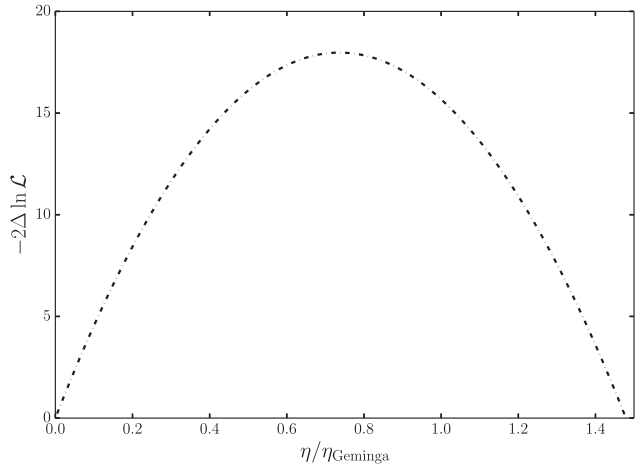

FIG. 4. The change to the log-likelihood (relative to no gamma-ray emission, $\eta_{\rm MSP} = 0$) as a function of the efficiency for very high-energy gamma-ray production, assuming that all 37 MSPs have the same efficiency. The best-fit value of $\eta_{\rm MSP} = 0.74\eta_{\rm Geminga}$ improves the fit by $2\Delta \ln \mathcal{L} = 17.97$, corresponding to a statistical preference of 4.24σ. At the 2σ level, our fit prefers $\eta_{\rm MSP} = (0.39 - 1.08) \times \eta_{\rm Geminga}$.

The results of our joint likelihood is shown in Fig. 4. Specifically, by utilizing the values in Fig. 3, we can translate our results between the expected flux of each source at a given declination, and the expected TS of that source at a given flux. Because this relationship is extremely tightly correlated, these translations invoke very little error. We then compose a joint-likelihood of each individual source, effectively moving up and down the normalization of the solid line in Fig. 2 to obtain a best-fit value and corresponding improvement to the log-likelihood fit.

Under the assumption of a common gamma-ray efficiency for the 37 MSPs in our sample, we find that the HAWC data is best fit for an efficiency of $\eta_{\rm MSP} = 0.74\eta_{\rm Geminga}$, which improves the fit by $2\Delta \ln \mathcal{L} = 17.97$ over the hypothesis of no gamma-ray emission from these sources, corresponding to a statistical preference of 4.24σ. At the 2σ level, our fit prefers an efficiency in the range of $\eta_{\rm MSP} = (0.39\text{–}1.08) \times \eta_{\rm Geminga}$. Stated more generically, this indicates that our model prefers a model where MSPs emit TeV photons with an efficiency that is 74% of the observed Geminga efficiency at more than 4σ compared to a null model where MSPs do not emit TeV γ-rays.

Efforts to compare our results to those presented in Ref. [34] are complicated by the fact that the 2HWC and 3HWC online tools have employed different spectral indices, and thus can yield somewhat divergent results. That being said, we note that of the four MSPs found in Ref. [34] to exhibit TS > 2, two have significantly larger TS values in this study (J0030 + 0451 and J1939 + 2134), while one has somewhat lessened (J1959 + 2048).

Thus far in our analysis, we have intrinsically assumed that each MSP produces a TeV halo with the same efficiency, η. It seems likely, however, that there will be some degree of pulsar-to-pulsar scatter in this quantity, with some MSPs featuring larger or smaller values of η. With this in mind, we have repeated our analysis following the approach described in Ref. [37], allowing the distribution of the values of η (equivalent to β in Ref. [37]) to be drawn from a log-normal distribution. In doing this, we have found that including a 0.5 decade ($\sigma \sim 0.5$) pulsar-to-pulsar variation in η does, in fact, improve our fit somewhat, although only with a modest statistical significance of $\sim 1.5\sigma$. In light of this, we cannot at this time make any detailed statements regarding the likely distribution of η.

As presented in the preceding paragraphs, the statistical significance of our results depends on the assumption that the backgrounds are normally distributed. This is not, in fact, the case, and non-Gaussian tails are empirically observed in the distribution of TS values of random sky locations obtained using the 3HWC Survey Tool. With this in mind, we have constructed a control group by measuring the TS values of a large number of sky locations using the 3HWC Survey Tool. These "blank sky" locations were selected such that they are each within HAWC's field-of-view and located no closer than $0.5° \times [\ln(\mathrm{TS}_{\rm 3HWC})]^{1/2}$ from any source in the 3HWC catalog. To make this collection of sky locations most closely reflect the characteristics of our MSP sample, we have divided our 37 sources into 10° bins in RA and Dec, and drawn control group sky locations from this statistical distribution of bins (and using a flat distribution within each 10° increment). We have also randomly selected the distance to each control group source (this determines which angular template is

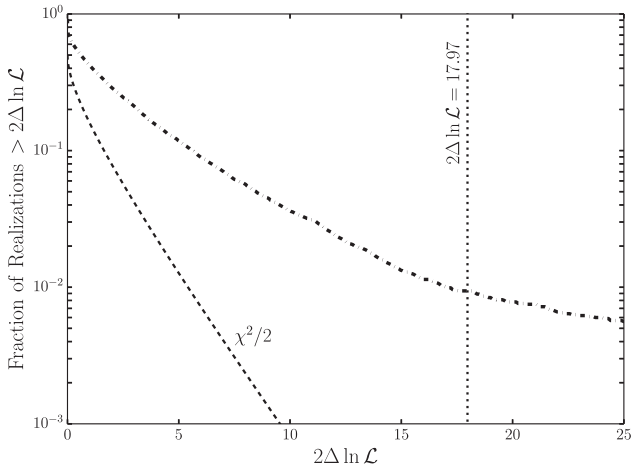

FIG. 5. The fraction of 10,000 randomly selected control group realizations that yield evidence for very high-energy gamma-ray emission at a given statistical significance (solid curve). This is compared to the predictions expected from a normal distribution, labeled $\chi^2/2$. From among this collection of 10,000 control group samples, only 94 (0.94%) favored a nonzero gamma-ray flux with as much statistical significance ($2\Delta \ln \mathcal{L} = 17.97$) as the collection of 37 MSPs considered in this study.

used in the 3HWC Survey Tool), weighted by the distances to the 37 MSPs in our sample. From this distribution we generated 10,000 sets of 37 sky locations (and angular templates). From among this collection of 10,000 control group samples, only 94 (0.94%) favored a nonzero gamma-ray flux at a level exceeding the statistical significance as our 37 MSPs (see Fig. 5). We note that this bootstrapping analysis includes mock MSP locations that are both near the galactic plane, or are relatively close to nearby 3HWC sources, providing a representative background model which should account for statistical upward fluctuations that may be play a role in the flux determinations of some MSPs, as discussed earlier, for example in the case of MSP J1939 + 2134.

IV. IMPLICATIONS FOR THE GALACTIC CENTER GAMMA-RAY EXCESS

In this section, we discuss the implications of our current results for our understanding of the Galactic center excess, reinterpreting these new results in the context of previous work in the field. Specifically, we note that a bright and statistically significant excess of GeV-scale gamma rays from the region surrounding the Galactic Center has been identified in data collected by the Fermi Gamma-Ray Space Telescope [30,38] (for earlier work, see Refs. [29,39–45]). The fact that the spectrum, morphology, and intensity of this excess are each consistent with the expectations from annihilating dark matter particles has generated a great deal of interest [46–67]. The primary alternative explanation for this signal is that these gamma rays are instead generated by a large population of centrally concentrated and unresolved MSPs [29,31–33,40–43].

To date, no individual MSPs have been detected in the inner galaxy. Despite this, interest in the possibility that MSPs could generate this signal grew considerably in 2015, when two groups claimed to find evidence of small-scale power in the excess, favoring point source interpretations of this signal [32,33]. It was subsequently shown, however, that analyses making use of non-Poissonian templates (as were used in Ref. [32]) tend to misattribute smooth gamma-ray signals to point source populations, especially in the presence of imperfectly modeled diffuse backgrounds [68–70]. Similarly, it was shown in Ref. [71] that the small-scale power identified in the wavelet-based analyses of Ref. [33] is not attributable to the gamma-ray excess. At this time, the Fermi data cannot be said to favor a pulsar interpretation of this signal, as was previously claimed. Instead, this class of analyses can, at present, only be used to place constraints on the luminosity function of any point source population that might be present in the inner galaxy (see, for example, Refs. [72,73]).

More recently, claims have been made that the gamma-ray excess is better fit by a template that reflects the spatial distribution of stars in the Milky Way's bulge and bar than that of a spherically symmetric, dark matter-like template [74–77]. If confirmed, this would favor scenarios in which the gamma-ray excess is generated by MSPs or other point sources which trace the stellar distribution of the inner galaxy. The conclusions of these studies, however, are highly sensitive to the details of the background model adopted, and on the spatial tails of the excess. Given the uncertainties associated with these factors, it is far from clear which of these templates better resembles the morphology of the actual gamma-ray excess. We also note that recent studies by Di Mauro [78] and Cholis *et al.* [79] have reached very different conclusions to those presented in Refs. [74–77], bringing the preference for a bulge-like morphology further into doubt.

Several arguments have been leveled against MSP interpretations of the gamma-ray excess. First, if the central MSP population exhibited the same gamma-ray luminosity function as those observed in the disk [80–82] and globular cluster populations [83] of the Milky Way, Fermi should have already resolved $\sim\mathcal{O}(10\text{–}20)$ individual MSPs from the inner region of the Galaxy. In contrast, no such sources have been identified. Furthermore, the number of low-mass x-ray binaries observed in the inner galaxy suggests that no more than ∼4%–23% of the gamma-ray excess originates from MSPs [84] (see also, Ref. [80]).

Looking forward, there are a number of ways in which this situation could be substantially clarified. First, if MSPs are responsible for this excess, a significant number of these objects should be detectable with upcoming large-area radio surveys [85]. Second, if gamma-ray emission with the same spectral shape as observed from the Galactic Center is detected from one or more dwarf galaxies, this would provide a strong confirmation of the dark matter interpretation of this signal [86]. This appears particularly promising in light of the large number of dwarf galaxies that the Rubin Observatory is anticipated to discover. Third, if AMS-02 were to robustly confirm the presence of the cosmic-ray antiproton excess reported in Refs. [87–90], this would also serve to bolster the dark matter interpretation of the Galactic Center excess.

The results of this study have significant bearing on the question of the origin of the Galactic Center gamma-ray excess. In particular, if MSPs generate TeV halos with a Geminga-like efficiency, as our results indicate is the case, then any MSPs which contribute to the Fermi excess should also produce significant emission at very-high energies. In our previous study [34], we showed that if there are enough MSPs in the inner galaxy to produce the Fermi excess, their TeV emission (if produced with a Geminga-like efficiency) would exceed or saturate that observed by HESS from the innermost 0.5° around the Galactic Center [91]. While this TeV emission could plausibly be suppressed by the presence of strong magnetic fields, this would result in more radio synchrotron emission than is observed [34]. While we do not repeat here the calculations which support this

conclusion, the results shown in Figs. 4 and 5 of Ref. [34] (see also, Ref. [92]) apply if MSPs have Geminga-like TeV halos, as is indicated by results presented in this study.[5]

Lastly, we note that while measurements from HESS currently place strong constraints on the TeV flux (and thus the total number of TeV-emitting MSPs) within the inner few degrees around the Galactic Center, this region is somewhat smaller than the ∼5–10° region in which the GeV excess is most pronounced. Fortunately, upcoming observations by the Cherenkov Telescope Array (CTA) [94] will be able to produce high-resolution maps of the very high-energy gamma-ray emission from the entire inner galaxy. By either identifying the TeV halo emission from a large MSP population, or by placing strong constraints on the number of MSPs present in the inner galaxy, CTA is expected to be able to clarify this situation considerably [95].

V. SUMMARY AND CONCLUSIONS

In this study (which builds on the work presented in Ref. [34] by utilizing the more recent 3HWC catalog along with better models for the diffuse background), we have presented significant evidence that millisecond pulsars (MSPs), like young and middle-aged pulsars, produce and are surrounded by TeV halos. Using data provided by the HAWC Collaboration, we performed a stacked likelihood analysis of 37 MSPs selected for their spindown power and proximity, finding evidence that these objects produce very high-energy gamma-ray emission, with a statistical significance corresponding to $(2\Delta \ln \mathcal{L})^{1/2} = 4.24$. Using sets of randomly selected sky locations as a control group, we found that less than 1% of such realizations yielded as much statistical significance. These statistical results exceed that of previous modeling efforts and provide increased evidence that MSPs may produce extended TeV halos.

Our analysis indicates (with results consistent with [34]) that MSPs produce very high-energy gamma-ray emission with a similar efficiency to that observed from the Geminga TeV-halo, $\eta_{\rm MSP} = (0.39 - 1.08) \times \eta_{\rm Geminga}$. This conclusion is also supported by a flattening in the observed correlation between the far-infrared and radio luminosities of old star-forming galaxies [96], which may be indicative of extra synchrotron emission powered by e^+e^- acceleration within the population of MSPs in old, quiescent galaxies.

This result has important implications for the origin of Galactic Center gamma-ray excess, as it indicates that if MSPs are responsible for the excess observed by Fermi, then they should also produce TeV-scale emission at a level that would exceed or saturate that observed from the inner galaxy by HESS. We look forward to observations by CTA, which should be able to either clearly identify the TeV halo emission from a large MSP population, or strongly constrain the number of MSPs that are present in the inner galaxy. Additionally, our models indicate that MSPs may produce a non-negligible local e^+e^- flux, though studies of the MSP population [22] indicate that the total lepton power from these sources would be unable to explain more than a few percent of the positron excess observed by PAMELA [97] and AMS-02 [98]. Young pulsars remain the most likely source for the vast majority of the positron excess [5].

Finally, we note that future observations of MSPs at TeV energies, including upcoming HAWC and LHAASO data, as well as targeted observations by H.E.S.S., VERITAS or CTA, could provide concrete evidence capable of confirming, or ruling out the TeV halo hypothesis presented here. Moreover, we note that additional spectral information produced by Atmospheric Cherenkov Telescopes may be capable of verifying the leptonic nature of any observed excesses, and ruling out interpretations that rely on background astrophysical contamination.

[5]Similar conclusions were reached in Ref. [93], in particular in the case that TeV halos inject electrons and positrons with a spectral index similar to that observed from Geminga and Monogem, $\Gamma \sim -1.5$ to -2.

ACKNOWLEDGMENTS

D. H. is supported by the Fermi Research Alliance, LLC under Contract No. DE-AC02-07CH11359 with the U.S. Department of Energy, Office of High Energy Physics. T. L. is supported by the Swedish Research Council under Contract No. 2019-05135, the Swedish National Space Agency under Contract No. 117/19, and the European Research Council under Grant No. 742104.

[1] A. Albert *et al.* (HAWC Collaboration), Astrophys. J. **905**, 76 (2020).
[2] A. Abeysekara *et al.*, Astrophys. J. **843**, 40 (2017).
[3] A. Abeysekara *et al.* (HAWC Collaboration), Science **358**, 911 (2017).
[4] A. A. Abdo *et al.*, Astrophys. J. Lett. **700**, L127 (2009).
[5] D. Hooper, I. Cholis, T. Linden, and K. Fang, Phys. Rev. D **96**, 103013 (2017).
[6] D. Hooper and T. Linden, Phys. Rev. D **98**, 083009 (2018).
[7] G. Johannesson, T. A. Porter, and I. V. Moskalenko, Astrophys. J. **879**, 91 (2019).

[8] M. Di Mauro, S. Manconi, and F. Donato, Phys. Rev. D **101**, 103035 (2020).
[9] R.-Y. Liu, H. Yan, and H. Zhang, Phys. Rev. Lett. **123**, 221103 (2019).
[10] T. Linden, K. Auchettl, J. Bramante, I. Cholis, K. Fang, D. Hooper, T. Karwal, and S. W. Li, Phys. Rev. D **96**, 103016 (2017).
[11] T. Sudoh, T. Linden, and J. F. Beacom, Phys. Rev. D **100**, 043016 (2019).
[12] T. Sudoh, T. Linden, and D. Hooper, J. Cosmol. Astropart. Phys. 08 (2021) 010.
[13] G. Giacinti, A. M. W. Mitchell, R. López-Coto, V. Joshi, R. D. Parsons, and J. A. Hinton, Astron. Astrophys. **636**, A113 (2020).
[14] S.-H. Wang, K. Fang, X.-J. Bi, and P.-F. Yin, Phys. Rev. D **103**, 063035 (2021).
[15] M. Di Mauro, S. Manconi, M. Negro, and F. Donato, Phys. Rev. D **104**, 103002 (2021).
[16] G. Principe, A. M. W. Mitchell, S. Caroff, J. A. Hinton, R. D. Parsons, and S. Funk, Astron. Astrophys. **640**, A76 (2020).
[17] A. Smith (HAWC Collaboration), Proc. Sci., ICRC2019 (**2020**) 797.
[18] A. Albert *et al.* (HAWC Collaboration), Astrophys. J. Lett. **911**, L27 (2021).
[19] H. Abdalla *et al.* (HESS Collaboration), Astron. Astrophys. **612**, A1 (2018).
[20] H. Abdalla *et al.* (HESS Collaboration), Astron. Astrophys. **612**, A2 (2018).
[21] A. Abeysekara *et al.* (HAWC Collaboration), Phys. Rev. Lett. **124**, 021102 (2020).
[22] C. Venter, A. Kopp, A. K. Harding, P. L. Gonthier, and I. Büsching, Astrophys. J. **807**, 130 (2015).
[23] W. Bednarek, J. Sitarek, and T. Sobczak, Mon. Not. R. Astron. Soc. **458**, 1083 (2016).
[24] C. Venter, A. Kopp, A. K. Harding, P. L. Gonthier, and I. Büsching, Proc. Sci., ICRC2015 (**2016**) 462.
[25] L. Sironi and A. Spitkovsky, Astrophys. J. **741**, 39 (2011).
[26] B. M. Gaensler and P. O. Slane, Annu. Rev. Astron. Astrophys. **44**, 17 (2006).
[27] C. Evoli, T. Linden, and G. Morlino, Phys. Rev. D **98**, 063017 (2018).
[28] K. Fang, X.-J. Bi, and P.-F. Yin, Mon. Not. R. Astron. Soc. **488**, 4074 (2019).
[29] D. Hooper and L. Goodenough, Phys. Lett. B **697**, 412 (2011).
[30] T. Daylan, D. P. Finkbeiner, D. Hooper, T. Linden, S. K. N. Portillo, N. L. Rodd, and T. R. Slatyer, Phys. Dark Universe **12**, 1 (2016).
[31] K. N. Abazajian, J. Cosmol. Astropart. Phys. 03 (2011) 010.
[32] S. K. Lee, M. Lisanti, B. R. Safdi, T. R. Slatyer, and W. Xue, Phys. Rev. Lett. **116**, 051103 (2016).
[33] R. Bartels, S. Krishnamurthy, and C. Weniger, Phys. Rev. Lett. **116**, 051102 (2016).
[34] D. Hooper and T. Linden, Phys. Rev. D **98**, 043005 (2018).
[35] R. N. Manchester, G. B. Hobbs, A. Teoh, and M. Hobbs, Astron. J. **129**, 1993 (2005).
[36] M. Di Mauro, S. Manconi, and F. Donato, Phys. Rev. D **100**, 123015 (2019).
[37] D. Hooper, T. Linden, and A. Lopez, J. Cosmol. Astropart. Phys. 08 (2016) 019.
[38] M. Ackermann *et al.* (Fermi-LAT Collaboration), Astrophys. J. **840**, 43 (2017).
[39] L. Goodenough and D. Hooper, arXiv:0910.2998.
[40] D. Hooper and T. Linden, Phys. Rev. D **84**, 123005 (2011).
[41] K. N. Abazajian and M. Kaplinghat, Phys. Rev. D **86**, 083511 (2012); **87**, 129902(E) (2013).
[42] D. Hooper and T. R. Slatyer, Phys. Dark Universe **2**, 118 (2013).
[43] C. Gordon and O. Macias, Phys. Rev. D **88**, 083521 (2013); **89**, 049901(E) (2014).
[44] F. Calore, I. Cholis, and C. Weniger, J. Cosmol. Astropart. Phys. 03 (2015) 038.
[45] M. Ajello *et al.* (Fermi-LAT Collaboration), Astrophys. J. **819**, 44 (2016).
[46] A. Berlin, D. Hooper, and S. D. McDermott, Phys. Rev. D **89**, 115022 (2014).
[47] A. Berlin, P. Gratia, D. Hooper, and S. D. McDermott, Phys. Rev. D **90**, 015032 (2014).
[48] M. Abdullah, A. DiFranzo, A. Rajaraman, T. M. P. Tait, P. Tanedo, and A. M. Wijangco, Phys. Rev. D **90**, 035004 (2014).
[49] D. Hooper, N. Weiner, and W. Xue, Phys. Rev. D **86**, 056009 (2012).
[50] A. Martin, J. Shelton, and J. Unwin, Phys. Rev. D **90**, 103513 (2014).
[51] S. D. McDermott, Phys. Dark Universe **7–8**, 12 (2015).
[52] M. Cahill-Rowley, J. Gainer, J. Hewett, and T. Rizzo, J. High Energy Phys. 02 (2015) 057.
[53] D. Hooper, Phys. Rev. D **91**, 035025 (2015).
[54] J. Liu, N. Weiner, and W. Xue, J. High Energy Phys. 08 (2015) 050.
[55] A. Achterberg, S. Amoroso, S. Caron, L. Hendriks, R. Ruiz de Austri, and C. Weniger, J. Cosmol. Astropart. Phys. 08 (2015) 006.
[56] A. Berlin, S. Gori, T. Lin, and L.-T. Wang, Phys. Rev. D **92**, 015005 (2015).
[57] J. M. Cline, G. Dupuis, Z. Liu, and W. Xue, Phys. Rev. D **91**, 115010 (2015).
[58] G. Bertone, F. Calore, S. Caron, R. Ruiz, J. S. Kim, R. Trotta, and C. Weniger, J. Cosmol. Astropart. Phys. 04 (2016) 037.
[59] N. Fonseca, L. Necib, and J. Thaler, J. Cosmol. Astropart. Phys. 02 (2016) 052.
[60] K. Freese, A. Lopez, N. R. Shah, and B. Shakya, J. High Energy Phys. 04 (2016) 059.
[61] A. Alves, S. Profumo, F. S. Queiroz, and W. Shepherd, Phys. Rev. D **90**, 115003 (2014).
[62] P. Agrawal, B. Batell, D. Hooper, and T. Lin, Phys. Rev. D **90**, 063512 (2014).
[63] E. Izaguirre, G. Krnjaic, and B. Shuve, Phys. Rev. D **90**, 055002 (2014).
[64] S. Ipek, D. McKeen, and A. E. Nelson, Phys. Rev. D **90**, 055021 (2014).
[65] Y.-L. Tang and S.-h. Zhu, J. High Energy Phys. 03 (2016) 043.
[66] M. Escudero, D. Hooper, and S. J. Witte, J. Cosmol. Astropart. Phys. 02 (2017) 038.
[67] M. Escudero, S. J. Witte, and D. Hooper, J. Cosmol. Astropart. Phys. 11 (2017) 042.

[68] R. K. Leane and T. R. Slatyer, Phys. Rev. Lett. **123**, 241101 (2019).
[69] R. K. Leane and T. R. Slatyer, Phys. Rev. D **102**, 063019 (2020).
[70] R. K. Leane and T. R. Slatyer, Phys. Rev. Lett. **125**, 121105 (2020).
[71] Y.-M. Zhong, S. D. McDermott, I. Cholis, and P. J. Fox, Phys. Rev. Lett. **124**, 231103 (2020).
[72] F. List, N. L. Rodd, G. F. Lewis, and I. Bhat, Phys. Rev. Lett. **125**, 241102 (2020).
[73] F. Calore, F. Donato, and S. Manconi, Phys. Rev. Lett. **127**, 161102 (2021).
[74] O. Macias, C. Gordon, R. M. Crocker, B. Coleman, D. Paterson, S. Horiuchi, and M. Pohl, Nat. Astron. **2**, 387 (2018).
[75] R. Bartels, E. Storm, C. Weniger, and F. Calore, Nat. Astron. **2**, 819 (2018).
[76] O. Macias, S. Horiuchi, M. Kaplinghat, C. Gordon, R. M. Crocker, and D. M. Nataf, J. Cosmol. Astropart. Phys. 09 (2019) 042.
[77] M. Pohl, O. Macias, P. Coleman, and C. Gordon, arXiv: 2203.11626.
[78] M. Di Mauro, Phys. Rev. D **103**, 063029 (2021).
[79] I. Cholis, Y.-M. Zhong, S. D. McDermott, and J. P. Surdutovich, arXiv:2112.09706 [Phys. Rev. D (to be published)].
[80] I. Cholis, D. Hooper, and T. Linden, J. Cosmol. Astropart. Phys. 06 (2015) 043.
[81] D. Hooper and G. Mohlabeng, J. Cosmol. Astropart. Phys. 03 (2016) 049.
[82] R. Bartels, D. Hooper, T. Linden, S. Mishra-Sharma, N. L. Rodd, B. R. Safdi, and T. R. Slatyer, Phys. Dark Universe **20**, 88 (2018).
[83] D. Hooper and T. Linden, J. Cosmol. Astropart. Phys. 08 (2016) 018.
[84] D. Haggard, C. Heinke, D. Hooper, and T. Linden, J. Cosmol. Astropart. Phys. 05 (2017) 056.
[85] F. Calore, M. Di Mauro, F. Donato, J. W. T. Hessels, and C. Weniger, Astrophys. J. **827**, 143 (2016).
[86] A. Albert *et al.* (Fermi-LAT, DES Collaborations), Astrophys. J. **834**, 110 (2017).
[87] A. Cuoco, M. Krämer, and M. Korsmeier, Phys. Rev. Lett. **118**, 191102 (2017).
[88] M.-Y. Cui, Q. Yuan, Y.-L. S. Tsai, and Y.-Z. Fan, Phys. Rev. Lett. **118**, 191101 (2017).
[89] I. Cholis, T. Linden, and D. Hooper, Phys. Rev. D **99**, 103026 (2019).
[90] A. Cuoco, J. Heisig, L. Klamt, M. Korsmeier, and M. Krämer, Phys. Rev. D **99**, 103014 (2019).
[91] A. Abramowski *et al.* (H.E.S.S. Collaboration), Nature (London) **531**, 476 (2016).
[92] D. Hooper, I. Cholis, and T. Linden, Phys. Dark Universe **21**, 40 (2018).
[93] D. Song, O. Macias, and S. Horiuchi, Phys. Rev. D **99**, 123020 (2019).
[94] B. Acharya *et al.* (CTA Consortium Collaboration), *Science with the Cherenkov Telescope Array* (World Scientific Publishing, Singapore, 2018).
[95] O. Macias, H. van Leijen, D. Song, S. Ando, S. Horiuchi, and R. M. Crocker, Mon. Not. R. Astron. Soc. **506**, 1741 (2021).
[96] T. Sudoh, T. Linden, and J. F. Beacom, Phys. Rev. D **103**, 083017 (2021).
[97] O. Adriani, G. C. Barbarino, G. A. Bazilevskaya, R. Bellotti, M. Boezio, E. A. Bogomolov, L. Bonechi, and M. Bongi (PAMELA Collaboration), Phys. Rev. Lett. **105**, 121101 (2010).
[98] M. Aguilar, G. Alberti, B. Alpat, A. Alvino, G. Ambrosi, K. Andeen, H. Anderhub, L. Arruda *et al.* (AMS Collaboration), Phys. Rev. Lett. **110**, 141102 (2013).